

Au/InSb(110) interface profiles from synchrotron-radiation and polar-angle-dependent x-ray photoemission

Yoram Shapira,* F. Boscherini, C. Capasso, F. Xu, D. M. Hill, and J. H. Weaver

Department of Chemical Engineering and Materials Science, University of Minnesota, Minneapolis, Minnesota 55455

(Received 13 February 1987; revised manuscript received 27 July 1987)

High-resolution synchrotron-radiation photoemission and polar-angle-dependent x-ray photoemission have been used to examine the chemistry and atomic profile of the Au/InSb(110) interface. These results show considerable Au-induced disruption and atomic intermixing at low coverage. Mathematical simulations of the experimental polar profiles predict that the atomic densities of both In and Sb decrease exponentially with distance into the Au layer, with concentration gradients for Sb at both the buried interface and the surface due to Sb segregation. Comparisons with other Au-semiconductor interfaces suggest common interface behavior with differences related to substrate bond strengths and semiconductor atom solubilities in Au.

Among the III-V semiconductors, InSb has the narrowest energy gap (0.17 eV direct gap at 300 K) and is a prime material for infrared detection in the 3–5 μm range. Moreover, band-gap tunability is possible through ternary-compound superlattice formation. InSb has the technological advantage of having an extremely high electron mobility (78 000 cm^2/Vs at 300 K), thus making it suitable for fabrication of fast devices in the microwave region. Despite its importance, very little is known about the chemistry and physics of evolving metal-InSb interfaces—far less than is known about GaAs or InP, for example.^{1–5} The relatively weak In–Sb bond strength suggests that disruption of the semiconductor substrate would be larger for InSb interfaces than for GaAs or InP systems, even if reactive intermixing is slight. In this paper, we discuss the behavior of the Au/InSb(110) interface. As we will show, the Au/InSb interface is relatively wide, and Sb and In segregate to the Au surface and near surface (Sb segregation is much more pronounced).

Single-crystal bars of InSb oriented in the (110) direction were supplied by MCP Electronic Materials Ltd. (dimension $5 \times 5 \times 20 \text{ mm}^3$, Te doped at $3 \times 10^{15} \text{ cm}^{-3}$). High-quality clean surfaces were obtained by cleavage *in situ* at operating pressures of $\sim 5 \times 10^{11}$ Torr. Au was evaporated from resistively heated W wire baskets mounted 30–40 cm from the sample (pressure during deposition less than 2×10^{-10} Torr, typical rate 1 $\text{\AA}/\text{min}$). The deposition of Au was monitored with a quartz-crystal oscillator. We report the nominal coverage in angstroms where one monolayer (ML) of the InSb(110) surface would correspond to 1.14 \AA of Au if the Au layer were epitaxial.

Polar-angle-dependent x-ray photoemission measurements (PADXPS) were done with a Surface Science Instruments SSX-100-03 spectrometer mounted on a dual-chamber vacuum system designed for interface research.⁵ Photoelectrons were excited by a focused, monochromatized Al K_{α} x-ray beam (150 μm to 1 mm diameter) and were energy analyzed with a hemispheri-

cal analyzer using multichannel detection (pass energies between 25 and 150 eV). Spectra were collected for angles between 10° (grazing) and 90° (normal emission) with a half-angle of acceptance of $\sim 15^\circ$.

Synchrotron-radiation photoemission (SRPES) measurements were undertaken at the Aladdin storage ring at the Wisconsin Synchrotron Radiation Center using the Grasshopper Mark II monochromator and beam line. The nominal total instrumental resolution was 185 meV for both the In 4d core levels ($h\nu=60$ eV) and the Sb 4d core levels ($h\nu=75$ eV). The photoelectrons were energy analyzed with a double-pass cylindrical-mirror analyzer (10 eV pass energy).

In Fig. 1 we show normalized In and Sb 4d PADXPS spectra for normal and grazing emission for cleaved

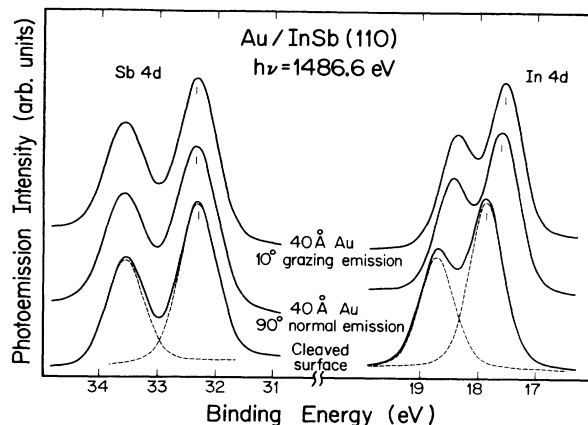


FIG. 1. Polar-angle-dependent XPS results for the In and Sb 4d core levels for cleaved InSb(110) and following the deposition of 40 \AA of Au. The dashed lines represent the spin-orbit-split 4d doublet. Spectra like these have been acquired for Au coverages of 10, 20, 40, 70, 100, and 150 \AA for polar angles of 10° , 20° , 30° , 40° , 50° , 60° , 75° , and 90° to characterize the evolving interface.

InSb(110) with and without a nominal Au coverage of 40 Å. The probe depth corresponds to $\sim 3\lambda \sin\theta$ where λ is the photoelectron mean free path (~ 17 Å for electrons of kinetic energy ~ 1450 eV) and θ is the photoelectron takeoff angle relative to the horizon. The 40-Å Au overlayer induced a binding-energy shift of -0.32 eV and line-shape sharpening. From the absence of a reacted component, we conclude that In atoms present in the near-surface region are dispersed in the Au matrix. There is no evidence for the formation of metallic In islands. For the Sb 4*d* spectra, there was a very slight shift to greater binding energy following the deposition of Au, together with a line-shape broadening because the probed region becomes more heterogeneous (the high-resolution, surface-sensitive SRPES results show a shift of -0.2 eV and line-shape sharpening). Again we find no evidence for compound formation, although the binding energy of Sb is relatively insensitive to its environment.

In Fig. 2 we show the results of the normalized In 4*d* photoemission intensities measured for nominal Au coverages of 10, 20, and 40 Å. Analogous results for Sb are given for Au coverages of 40, 70, 100, and 150 Å. These were obtained from the PADXPS spectra with the integrated core-level emission at each coverage and angle

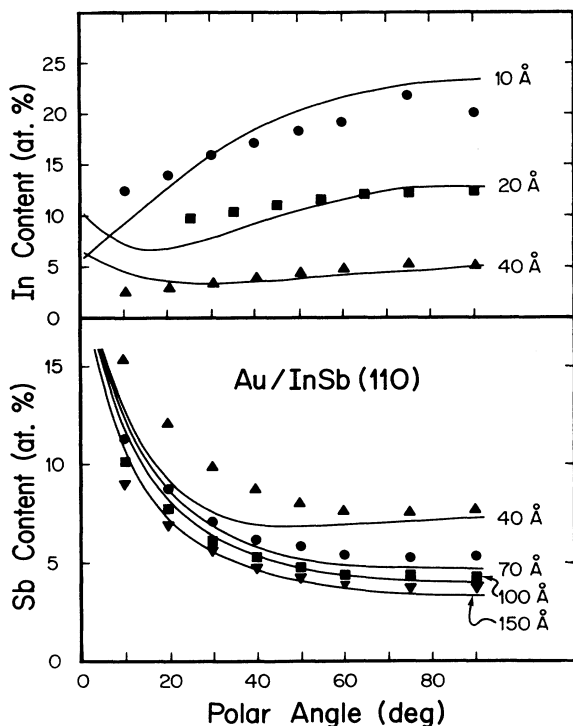


FIG. 2. In and Sb content within the probing region as a function of the polar angle with respect to the surface derived from the XPS core-level results. These values are measured intensities normalized to their relative photoionization cross sections and to the total normalized intensities. The solid curves are the theoretical fittings following a simple distribution model described in the text and discussed in detail in Refs. 8 and 9.

normalized to the corresponding emission of the clean surface. Quantitative analysis required the normalization of the integrated In 4*d*, Sb 4*d*, and Au 4*f* emission to their relative photoionization cross sections at $h\nu=1486.6$ eV, as discussed in detail elsewhere.^{6,7} As a result, we are able to determine the atomic concentration of In and Sb within the probed region as the probe depth (polar angle) is varied. From the substantial Sb 4*d* emission for Au coverages of 150 Å, we can conclude that Sb atoms are present in the overlayer. The PADXPS results show that the Sb emission increases at grazing angles for all coverages of Au, providing evidence for surface and near-surface segregation rather than uniform mixing. In contrast, the emission from In decreases rapidly with coverage and is below the level of detectability when the overlayer is 70 Å thick.

To obtain more details about the initial stages of evolution, we conducted synchrotron-radiation photoemission studies of the evolving Au/InSb interface. The Sb 4*d* results shown in Fig. 3 for representative Au coverages reveal a gradual shift to higher binding energy and a line-shape sharpening as the range of chemically distinct environments within the probe depth diminished [total shift 0.25 eV, full width at half maximum (FWHM) reduction from 0.75 to 0.61 eV, $\lambda\sim 4$ Å]. Significantly, no energetically shifted shoulder appears, in contrast to what occurs at reactive interfaces where shifted components represent specific interface compounds.⁵ These results indicate that dilution of semiconductor atoms in the growing Au overlayer starts at very low coverage. Similar behavior is observed for In where the total 4*d* shift was -0.28 eV and the FWHM decreased from 0.66 to 0.55 eV. The binding energies of the cation (anion) core levels decrease (increase) as the

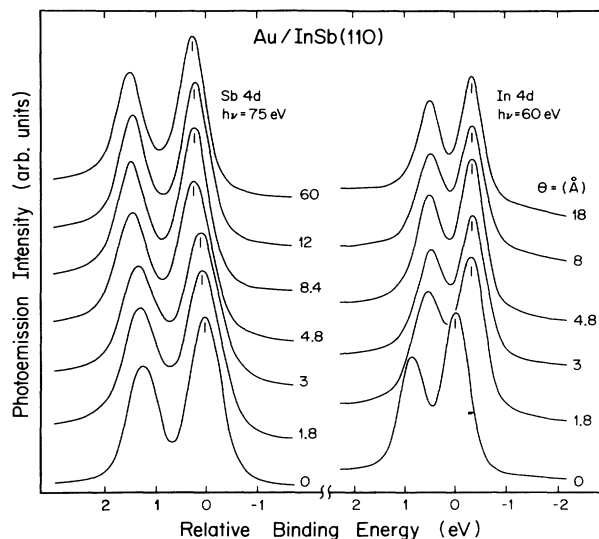


FIG. 3. Representative high-resolution, surface-sensitive photoemission results for In 4*d* and Sb 4*d*. There is no evidence for Au-Sb compound formation, but significant amounts of Sb persist in the probed region. The In 4*d* core-level shift of -0.32 eV reflects the dilution of In in the Au matrix.

final bonding configuration is reached. This corresponds to In dilution in Au and Sb segregation in the surface and near-surface regions.

Additional information about the growth morphology of the interface can be extracted from the attenuation curves shown in Fig. 4. At low coverages, there is a drop in intensity for both In and Sb. By 2 Å coverage, however, the Sb emission increases and its behavior deviates sharply from that of In. These highly-surface-sensitive measurements show that the emission from dissociated Sb exceeds that of the clean surface by $\Theta = 12$ Å, reaches a maximum near 30 Å, and decreases gradually with successive deposition of Au. This demonstrates the segregation of large amounts of Sb to the surface itself and shows the development of the final-state concentration profile. The gradual decrease above ~ 30 Å is consistent with the dissolution of Sb in the Au layer. In this same coverage range, the In intensity decays monotonically, first with a characteristic rate of ~ 5 Å but then more slowly. This shows that the amount of In in the probed region decreases quickly, consistent with the higher solubility of In in Au, the expectation that limited Au-In bonding might occur close to the interface, and the reduced disruption of the substrate after $\Theta \sim 5$ Å.

A physical picture of atomic diffusion and segregation can be developed from these results. Au adatoms initially disrupt In—Sb bonds and Au, In, and Sb atoms form an intermixed region. As the Au overlayer thickens, most of the dissociated atoms are trapped near the buried interface or are expelled to the surface region because of their low solubility in Au. The segregated layer "floats" because a minimum-energy configuration can be

achieved locally by the expulsion of the solute. Quantitative fitting of these results has been done by assuming exponential concentration profiles with the concentrations of In and Sb decaying into the Au film from the buried interface at low coverage and with distributions showing a double profile because of the segregation of Sb at the surface. Such fitting is discussed in detail in Refs. 6 and 7. In the center of the film, the distributions are determined by solid solubilities. For our thick Au overlayers (~ 100 Å), we have found the amount of In and Sb diluted in Au to be ~ 1 and ~ 0.3 at. %, respectively, in good agreement with the solubilities reported in the literature.⁸ The total amount of dissociated In and Sb within the Au films was the equivalent of ~ 5 ML of the InSb(110) substrate, thus giving an estimate of the extent of substrate disruption at room temperature. The $1/e$ decay length from the surface is ~ 3 Å.

This simple concentration model cannot completely describe the low-coverage behavior for a complex evolving interface because of the assumption of an abrupt interface and because too little is known about the onset of the segregation. Since our mathematical description fixes the total number of disrupted semiconductor atoms (determined at high coverages), our fittings overestimate the released In and Sb during the initial stages of disruption. The model describes the interface best at high coverages.

PADXPS studies have been reported previously for Au/GaAs(100).⁶ Although similar Ga and As distributions were observed, the amount of substrate disruption was smaller (total amount ~ 2.3 ML). We associate this with the stability of the substrate bonds. For Au/InP(110), Shapira *et al.*⁹ recently found In and P segregation to the surface, together with small amounts dissolved in the Au matrix. Finally, reports for Au/Ge (Ref. 10) and Au/Si (Ref. 11) interfaces suggest surface segregation of Ge and Si and the persistence of a surface phase that appears to have a stoichiometry of Au_3Ge or Au_3Si . In light of the present results, we propose that these surface Ge and Si phases are bonding configurations associated with dissociated Ge and Si with a sharp concentration profile decaying from the surface into the Au layer. All these Au-semiconductor interface results indicate that Au deposition results in limited disruption. It seems likely that the mechanism controlling the subsequent interface evolution at room temperature is the same, with differences that can be understood by examining the different bond strengths and solubilities of the semiconductor atoms in the Au overlayer. It should be pointed out, however, that the common behavior of these systems at room temperature will not necessarily be observed at temperatures high enough to cause reaction (e.g., AuGa compound formation) or morphology changes, as recently discussed by Williams and co-workers¹² based on thermodynamics and ternary phase diagrams.

This work was supported by the Office of Naval Research under Grant No. ONR N00014-87-K-0029. Part of the work was done at the Wisconsin Synchrotron Radiation Center which is supported by the National

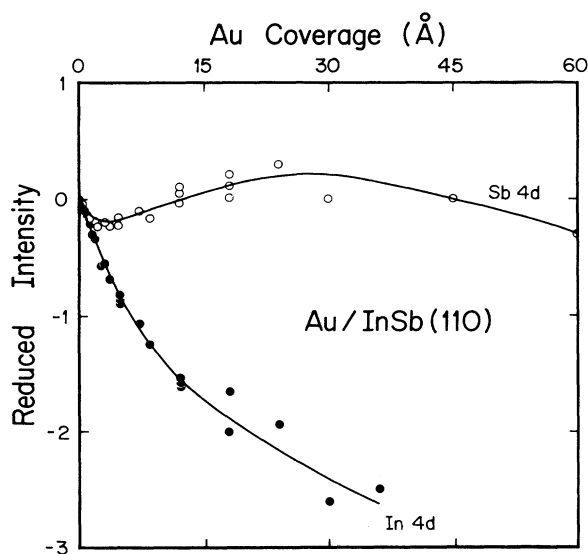


FIG. 4. Core-level attenuation profiles determined from the results of Fig. 3. Within the probed region of 12–15 Å, the In content decreases with coverage. In contrast, the Sb concentration first decreases, but the onset of segregation to the surface results in Sb 4d emission which exceeds that of the clean surface.

Science Foundation. Discussions with R. S. Williams are gratefully acknowledged. Y. Shapira is grateful to

the Belfer Center for Energy Research, Israel and the Kernforschungsanlage Jülich for their support.

*Permanent address: Faculty of Engineering, Tel Aviv University, Ramat-Aviv 69 978, Tel-Aviv, Israel.

¹L. J. Brillson, *Surf. Sci. Rep.* **2**, 123 (1982), and exhaustive references therein.

²W. G. Petro, T. Kendelewicz, I. Lindau, and W. E. Spicer, *Phys. Rev. B* **34**, 7089 (1986); T. Kendelewicz, W. G. Petro, I. Lindau, and W. E. Spicer, *Appl. Phys. Lett.* **44**, 1066 (1984); P. W. Chye, I. Lindau, P. Pianetta, C. M. Garner, C. Y. Su, and W. E. Spicer, *Phys. Rev. B* **18**, 5545 (1978), and references therein.

³R. H. Williams, *Contemp. Phys.* **23**, 329 (1982); *Surf. Sci.* **132**, 122 (1983).

⁴R. Ludeke, *Surf. Sci.* **132**, 143 (1983).

⁵J. J. Joyce, M. Grioni, M. del Giudice, M. W. Ruckman, F. Boscherini, and J. H. Weaver, *J. Vac. Sci. Technol. A* **5**, 2019 (1987). A photograph of the XPS spectrometer can be seen on the cover of *Phys. Today* **39**, No. 1 (1986).

⁶F. Xu, J. J. Joyce, M. W. Ruckman, H.-W. Chen, F. Boscherini, D. M. Hill, S. A. Chambers, and J. H. Weaver, *Phys. Rev. B* **35**, 2375 (1987).

⁷F. Xu, Yoram Shapira, D. M. Hill, and J. H. Weaver, *Phys. Rev. B* **35**, 7417 (1987).

⁸S. E. R. Hiscocks and W. Hume-Rothery, *Proc. R. Soc. London Ser. A* **282**, 318 (1964). The solubility of In in Au was reported to be 12.7 at. % at 963 K and 9 at. % at 373 K. M. Hansen, *Constitution of Binary Alloys* (McGraw-Hill, New York, 1958), quotes a value of ~ 8 at. % for the solid solubility of In in bulk Au at 300 K, while Sb was reported to be insoluble.

⁹Yoram Shapira, L. J. Brillson, A. D. Katnani, and G. Margaritondo, *Phys. Rev. B* **30**, 4586 (1984).

¹⁰M. W. Ruckman, J. J. Joyce, F. Boscherini, and J. H. Weaver, *Phys. Rev. B* **34**, 5118 (1986); P. Perfetti, A. D. Katnani, T.-X. Zhao, G. Margaritondo, O. Bisi, and C. Calandra, *J. Vac. Sci. Technol.* **21**, 628 (1982), and references therein for Au/Ge.

¹¹A. Franciosi, D. G. O'Neill, and J. H. Weaver, *J. Vac. Sci. Technol. B* **1**, 524 (1983); I. Abbati, L. Braicovich, A. Franciosi, I. Lindau, P. R. Skeath, C. Y. Su, and W. E. Spicer, *J. Vac. Sci. Technol.* **17**, 930 (1980), and references therein for Au/Si interfaces.

¹²J. H. Pugh and R. S. Williams, *J. Mater. Res.* **1**, 363 (1986); J. R. Lince, C. T. Tsai, and R. S. Williams, *ibid.* **1**, 537 (1986).